# NUCLEAR PHYSICS
## FOR CULTURAL HERITAGE

**A TOPICAL REVIEW BY**

the Nuclear Physics Division of the European Physical Society

**EDITED BY**

Anna Macková,
Douglas MacGregor,
Faiçal Azaiez,
Johan Nyberg,
and Eli Piasetzky

**INTRODUCTION BY**

Walter Kutschera

edp sciences

# NUCLEAR PHYSICS
## FOR CULTURAL HERITAGE

PUBLISHED BY

Nuclear Physics Division
of the European Physical Society,
October 2016

EDITED BY

Anna Macková, Douglas MacGregor,
Faiçal Azaiez, Johan Nyberg,
and Eli Piasetzky


DOI: 10.1071/978-2-7598-2091-7
ISBN: 978-2-7598-2091-7

COVER PICTURE

Early example of an external proton-beam PIXE set-up at the Ion Beam Center, Helmholtz Zentrum, Dresden - Rossendorf, Germany to study the color composition of the panel *Die vierzehn Nothelfer* by Lucas Cranach the Elder (1472-1553). Figure from C. Neelmeijer, W. Wagner, H.-P. Schramm, Diagnose von Kunstwerken am Teilchenbeschleuniger, *Restauro* 5 (1995) 326-329.

# TABLE OF CONTENTS

# TABLE OF CONTENTS

B. CONSTANTINESCU, L. GIUNTINI, N. GRASSI, V. HAVRÁNEK, M. JAKŠIĆ, J. KUČERA, F. LUCARELLI, A. MACKOVA, P.A. MANDÒ, M. MASSI, A. MIGLIORI, A. RE, Z. SIKETIĆ, F. TACCETTI, Ž. ŠMIT

# 2. ION BEAM ANALYTICAL METHODS

The use of accelerated ions has become an indispensable tool in the analysis of objects and materials in a wide range of scientific and technical studies. Historically, the first nuclear analytical method was Neutron Activation Analysis (NAA), based on principles discovered by Hevesy and Levi in 1936. Later, in the early 1960s, various types of Ion Beam Analyses (IBA) were invented and entered routine use. In the following decades nuclear analytical methods developed and matured, becoming highly valued analytic tools. The most recent development of IBA methods has been strongly related to progress in low energy accelerators, particle, X-ray and gamma-ray detectors and systems for accumulating and analysing experimental data.

## 2.1. BASIC PRINCIPLES OF ION BEAM ANALYSIS (IBA)

### NUCLEAR REACTION ANALYSIS (NRA)

The energy spectrum of charged particles produced in nuclear reactions is measured in NRA. The yield of nuclear reaction products is proportional to the reaction cross section (defined by the probability of a specific interaction) and the density of atoms in the sample. Energy losses by both the incident ions and the reaction products may be used for depth profiling of particular isotopes.

In Resonant Nuclear Reaction Analysis (RNRA) high peak cross sections at resonances give higher sensitivity. Energy loss by the incident ion can be used to determine depth profiles by resonance scanning. Nuclear reaction methods are suitable for identifying a range of isotopes from $^{1}H$ to $^{32}S$. The most frequently used reactions are (p,α), (d,p), and (d,α) in which incident protons, or deuterons, emit α-particles or protons. These reactions provide useful alternative methods for determining isotopes such as $^{2}H$, $^{12}C$, and $^{16}O$, compared with Rutherford Back-Scattering spectrometry (RBS) or Elastic Recoil Detection Analysis (ERDA).

Cross sections of 10–100 mb $sr^{-1}$ are observed for proton and deuteron-induced reactions on light isotopes, such as D, Li, Be, and B. Detection limits of the order of 10 $\mu g g^{-1}$ or even less are achievable with typical measuring times of the order of tens of minutes. Isotopes up to $^{32}S$ can be determined in heavier matrices at $mg g^{-1}$ levels depending on the maximum beam current that the sample can withstand. The use of glancing measurement geometries or heavy incident ions make possible depth profiling with typical resolutions at the surface of 10–100 nm.

As a result of ion beam irradiation of a material, two types of collision occur: inelastic collisions and elastic collisions.

In inelastic collisions two phases exist. In the first phase particles are emitted (NRA – Nuclear Reaction Analysis). This is followed in the second phase by the emission of γ-rays (PIGE – Particle Induced Gamma-ray Emission spectroscopy) or X-rays (PIXE – Particle Induced X-ray Emission spectroscopy) [4,5]. Nuclear reactions are isotope-specific (the reaction takes place on one particular isotope) with no direct relationship between the mass of the target nucleus and the energy of the emitted particles.

In elastic collisions two main phenomena are taking place: (i) the primary ion beam is back-scattered and is used in Rutherford Back-Scattering spectrometry (RBS) and (ii) lighter atomic nuclei can be ejected, recoiling from the heavier projectile ions. This is the principle of Elastic Recoil Detection Analysis (ERDA).

### PARTICLE INDUCED GAMMA-RAY EMISSON SPECTROSCOPY (PIGE)

PIGE or PIGME (particle-induced gamma-ray emission) is a versatile non-destructive analytical and depth profiling technique based on the (p,γ) reaction [6-9]. The γ-ray peaks are generally well isolated and the energy is high enough that no absorption correction is necessary.

The energies and intensities of the γ-ray lines indicate which elements are present and their respective amounts.

For protons with energies from 1 to 3 MeV, the best sensitivities are found for Li, B, F, Na, and Al. These elements can be determined simultaneously in many cases. Concentrations of F and Na can be obtained with uncertainties below 1%, in only a few minutes.

At proton energies above 3 MeV, the γ-ray emission from medium and heavy elements begins to compete with that from light elements. The highest cross sections are for light isotopes (A<30), which can be determined with a sensitivity of 1 $\mu g g^{-1}$ or less.

## PARTICLE INDUCED X-RAY EMISSION SPECTROSCOPY (PIXE)

PIXE uses X-ray emission for elemental analysis [4, 10-13]. Samples are irradiated by an ion beam from an accelerator and characteristic X-rays are then detected by Si(Li) or HPGe detectors. Ions, or protons, with energies of a few MeV ionise atoms in the sample and induce the emission of characteristic X-rays. PIXE is not a true nuclear technique, as the ionization of atoms by the ion beam and the subsequent emission of characteristic X-rays are purely atomic processes. The energy of the emitted X-rays is a monotonously increasing function of atomic number (Moseley's law). Hence, the energy of a peak in the X-ray spectrum is specific to a particular element and its intensity is proportional to the element's concentration.

As a result of its short measurement time, PIXE is the preferred method for the analysis of thin samples, *e.g.* from air filters, or for the automated analysis of large numbers of geological or archaeological samples. The concentrations of up to about 20 elements may be determined simultaneously. The low absolute detection limit, and good sensitivity, for elements such as S, P, Cl, K, Ca and Fe make PIXE of great importance in biological, archaeological and medical applications.

The X-ray yield depends on the number of atoms in the sample, the ionisation cross section, the intensity of the ion beam, the energy-dependent detection efficiency of the semiconductor detectors used, the composition of the sample and several other additional factors. The determination of an absolute concentration of an element in an unknown matrix is a complex problem. In practice, the evaluation of sample composition involves the use of standards and reference materials to determine the calibration curve of a particular measurement set-up. Depending on the sample type and measuring apparatus, the concentration of elements with Z>5 can be determined with sensitivities of 0.1–1 $\mu g g^{-1}$. PIXE has very low detection limits from $10^{-8}$ - $10^{-10}$ g in standard practice. This method is not used for elemental depth profiling, because of its low depth resolution.

The major advantage of PIXE's use of ions is a reduction in the background in comparison to that obtained when electrons are used as a probe (electron microprobe induced X-ray emission, EDX).

Differential PIXE (d-PIXE) is based on sequential measurements in the same locations so that protons reach different target depths. This is achieved either by variation of the incident proton angle or by variation of the proton energy. In either case, the strongest X-ray signal comes from the target surface, which largely screens out the contributions from inner layers. Sensitive numerical methods are then required to filter out these minute contributions. The results of the de-convolution procedure are concentration profiles, which can reach up to 10 μm below the target surface.

## RUTHERFORD BACK-SCATTERING SPECTROSCOPY (RBS)

In elastic collisions two main phenomena provide analytical information: (i) the energy transfer and (ii) the kinematics of elastic collisions between atomic nuclei and ions.

RBS is the most commonly used non-destructive nuclear method for elemental depth analysis of structures in the nanometer to micrometer thickness range [4,5,13-17]. Typical objects are thin surface films. The method is based on measurements of the energy spectra of several MeV ions (protons, singly charged helium $He^+$, or heavier ions) elastically scattered from solid samples. The samples are irradiated in an evacuated target chamber and the scattered particles are detected by semiconductor detectors. The energy spectra are evaluated using standard codes and information on the sample composition and the depth distribution of particular components is obtained. As a consequence of the scattering kinematics, the energy of the scattered particles increases monotonically as a function of the element mass.

The scattering cross section is proportional to the sample element atomic number squared. Thus the technique is particularly sensitive to heavier elements. The quantity of a particular element in the target is proportional to the number of scattered particles. The incident and scattered particles penetrating through the sample material lose energy progressively and the measured energy loss can be transformed into a depth using the known particle stopping powers in the sample material.

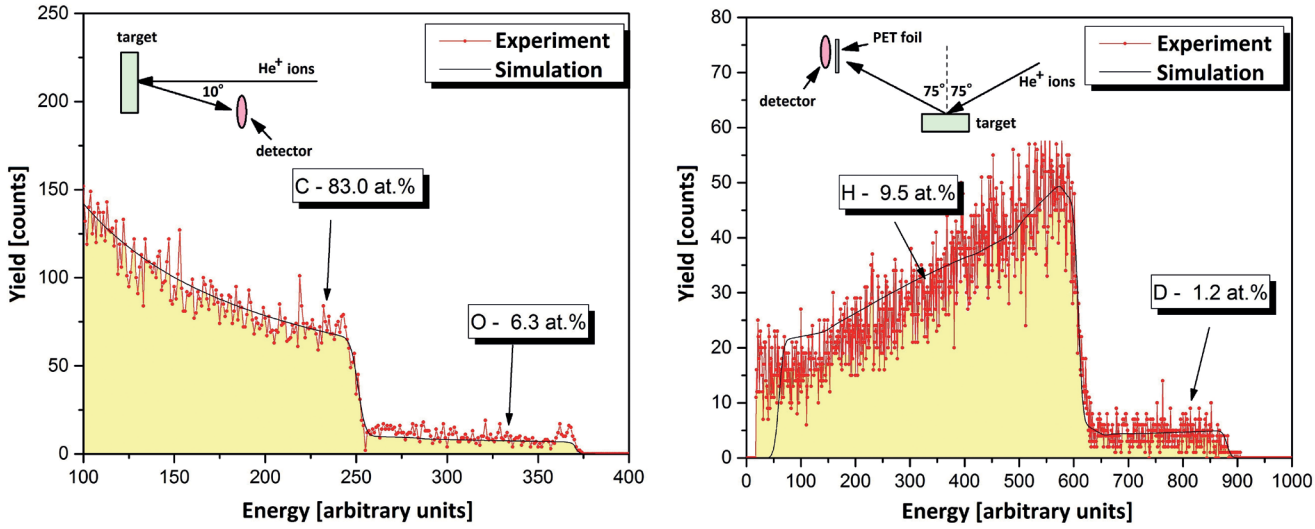


**Figure 2.1:** Complementary Rutherford Back-Scattering (RBS) and Elastic Recoil Detection Analysis (ERDA) analyses of deuterium-doped graphene based structures for depth profiling of heavy impurities, compositional studies and light dopants [18].

This makes it possible to determine the depth distribution of particular elements with a resolution as low as 10 nm. The sensitivity of RBS for the detection of trace impurities in bulk samples depends strongly on the sample composition and the experimental conditions. For heavy elements, in a light substrate, detection limits of about 0.01 atomic percent (at. %) can be achieved.

The major strengths of RBS are its relative simplicity, its non-destructive nature and the possibility of determining the detailed structure of samples. Figure 2.1 shows the combined analysis of light elements in graphene based structures using RBS and ERDA, which is described later in this section.

## RBS-CHANNELLING (RBS/C) SPECTROMETRY

RBS-channelling spectrometry is a method of investigating adventitious atoms located in the interstitial space of single crystals [19-21]. A beam of energetic ions is steered into open spaces (channels) between close-packed rows or planes of atoms in a crystal. Figure 2.2 shows the image of a single crystal rotated in a 2 MeV $He^+$ beam.

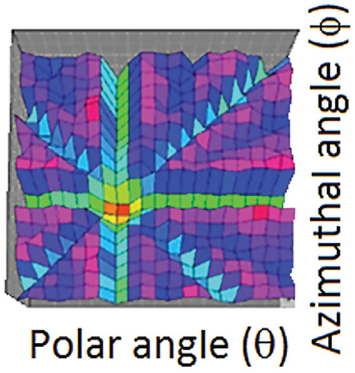


**Figure 2.2:** Image showing the RBS back-scattering yield of 2 MeV $He^+$ ions, from a single crystal as a function of the polar and azimuthal angles the crystal is rotated through.

The yield depends on the crystal orientation with respect to the ion beam and changes as the polar and azimuthal angles (θ, φ) between the crystal and the incident beam are varied. The observed intensities are reduced at angles corresponding to channelling between crystalline planes. The most prominent valley corresponds to an axial channel where the most ions are steered into the crystal and the back-scattered yield is very small. This direction corresponds to the orientation of the main crystallographic axis in the crystal.

The energy transfers or kinematics in elastic collisions between ions and atomic nuclei can give information about the composition and structure of the sample. The number of scattered particles measured by a detector can be converted to the concentration of a particular element in the target. The incident particle energy losses are much lower in the channelling regime compared to random incidence.

The energy spectrum of backscattered particles from an aligned crystal is dramatically different from that of non-aligned, randomly placed sample. In the aligned spectrum, the scattering yield from the bulk of the solid is reduced by around two orders of magnitude and a surface peak occurs. The presence of defects can significantly enhance the de-channelling yield comparing to a perfect crystal.

The backscattered yield from interstitial atoms does not exhibit the same decrease as that of the host crystal and can be used either for evaluation of the impurity position in a host crystal lattice or for the study of the displacement of host atoms from their lattice sites.

The major strength of RBS/C is an ability to determine the position of impurity atoms in a host crystal lattice. RBS/C is usually employed for the analysis of samples of known composition with the focus on impurity atoms or the number of defects.

### ELASTIC RECOIL DETECTION ANALYSIS (ERDA)

ERDA is one of the most useful ion beam analysis techniques for depth profiling of light elements [22-26]. A beam of energetic ions is directed towards the sample. When the incident ion has a heavier mass than the sample atoms, a light target atom may be knocked out and detected in a forward geometry using a semiconductor detector (see inset of Figure 2.1). Atoms recoiling from the surface appear at different energies depending on their mass and measuring arrangement.

The sensitivity of ERDA depends on the experimental arrangement and the system dependent background level. Typically 0.1 at. % of $^{1}H$ is observable and from 0.1 to 1 at. % of heavier atoms. Simple ERDA, using charged particle detectors with a stopping foil in front, has a depth resolution of typically 20–60 nm.

The stopping foil has to be thick enough to absorb primary ions elastically scattered from the sample. With higher mass projectiles, heavier elements such as N, O, and F can also be analysed by the simple ERDA technique. Absolute measurements of light atom content by ERDA are best achieved by using standards.

The arrangement with the stopping foil is not suitable for analyses of heavier elements using heavy projectiles; in this case heavy ion elastic recoil detection analysis (HIERDA) using ionisation chamber detectors and energy detectors, or time-of-flight techniques (TOF-ERDA), could be used to separate the masses and energies of the recoiling particles.

## 2.2. INSTRUMENTATION OF IBA

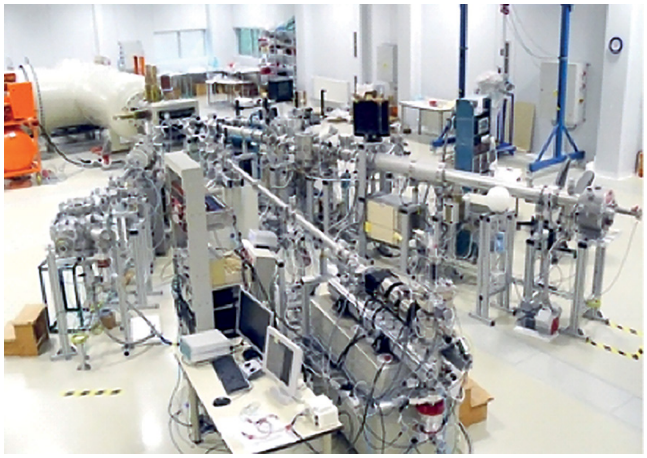

**Figure 2.3:** Tandetron accelerator with ion beam lines, vacuum chambers and detectors arrangement at the Center of Accelerators and Nuclear Analytical Methods (NPI CAS), Czech Republic, used for various nuclear analytical methods.

Standard equipment for IBA analysis comprises an electrostatic accelerator (see Figure 2.3), providing the ions (protons, deuterons, He and heavier ions) with energies from 0.5–50 MeV, with associated ion beam-lines and vacuum target chambers in which the samples under study are irradiated. The samples are mounted, several per load, on the table of a goniometer for precise positioning and orientation of the samples with respect to the incoming ion beam.

The products of ions interaction with sample atoms are registered by semi-conductor detectors with associated electronic devices for processing detector signals and data acquisition. An important part of the equipment is a device monitoring the beam intensity; Faraday cups, rotating vanes intersecting the beam or a thin wire mesh inserted in the beam are common techniques.

In general, the ion beam hits the sample at normal incidence. If the ion energy used is equal to the resonant energy in the RNRA method, the resonance reaction takes place on nuclei located at the surface. If the beam energy is higher than the resonant energy, the resonance occurs at depth, because of energy losses of the initial ions. By measuring the yield for a constant accumulated charge and varying the beam energy in small steps, the yield as a function of ion beam energy can be interpreted as the quantity of the element at various depths. That is, it provides the concentration depth profile. Incident ion energies from 0.5 to 2 MeV are most useful for minimising interference from reactions on heavy isotopes.

PIGE is mostly based on (p,γ), (p, p'γ), and (p,αγ) nuclear reactions induced by MeV protons where nuclear γ-rays are produced. In most cases, high purity germanium (HPGe) or scintillation detectors with multichannel acquisition systems are used for detection of γ-rays. The lower the incident ion energy, the fewer resonances are involved in ion–γ reactions and non-uniform angular distributions are more likely to be observed.

PIPS, or surface barrier detectors, are primarily used for detecting scattered ions in RBS and ERDA methods. A channelling RBS experiment requires a source of collimated high-energy ions from an accelerator, a detector for scattered particles (the same as for RBS), and an accurate crystal manipulator (goniometer). The goniometer is a crucial part of the equipment which allows the crystal axes to be aligned with the collimated particle beam.

ERDA relies on the ability to discriminate between forward scattered incident ions and recoiling light atoms. The typical experimental arrangement is a Mylar foil placed in front of the detector to block out the scattered incident ions but allow the lighter recoil atoms, which suffer considerably less energy loss, to pass through to the detector. Note that a 10 μm Mylar foil completely stops 2.6 MeV $He^{+}$ ions, but MeV recoil protons pass through with low-energy losses. Thus, $He^{+}$ ions are used for hydrogen profiling.

Heavy ion-ERDA (HIERDA) is able to analyse light and medium elements. Typically heavier ions such as $Cl^{n+}$ or $I^{n+}$ are used, with energies of tens of MeV. HIERDA needs an appropriate detection technique to distinguish the large

numbers of different particles that recoil simultaneously. The technique uses either the simultaneous measurement of the energies and velocities of the detected particles (TOF measurement) to separate the mass of recoils, or a gas-filled ionisation chamber for mass separation. The velocities in TOF measurements are determined by measuring the elapsed time between the detection of a particle in two sequential detectors placed a fixed distance apart. Gas filled detector measurements determine both the total energy and the energy loss of the recoiling particles. The signals from recoil elements, which overlap on a simple energy spectrum, are separated by their different energy loss rates.

### SPECIAL INSTRUMENTAL ARRANGEMENTS

In ion microprobe analysis, the samples are irradiated with an ion beam focused to a spot about 1 μm in diameter and standard IBA techniques (PIXE, RBS) are used for the characterisation of the part of the sample which is irradiated. By scanning the beam across the surface of the sample a 3D distribution of elements can, in principle, be determined with a nm depth resolution and a lateral resolution limited only by the size of the beam spot. For this purpose the signals from the detectors are recorded as a function of the current position of the beam spot. See Figures 2.4 and 2.5.

A fully equipped proton microprobe (PMP) chamber should include microscopes for transmission and reflective viewing of the specimen, a Si(Li) detector for detection of X-rays, surface barrier detectors for backward and forward collisions, and a detector for γ-rays. Charged particle beams are focused by means of magnetic or electrostatic lenses. The achievement of good spatial resolution requires a good ion optics design, high precision in fabrication, careful alignment, and elimination of sources of interference.

When the ion passes through a thin specimen, the beam transmitted in the forward direction includes some particles that scattered elastically off atomic nuclei, or lost energy as a result of interaction with electrons, as well as those particles that were not scattered. An image formed with this forward transmitted beam is referred to as a bright field image.

In order to measure the distribution of elements along a line, or map the elemental distribution over an area, the focused beam spot must be scanned and the detector signal recorded as a function of the displacement of the beam from its normal position. When a beam of ions scans an area of a specimen, the emitted radiation carries information in 3 degrees of freedom – the two scanning dimensions and the energy. Scanning ion microprobe (SIMP) and scanning proton microprobe are very useful techniques for in situ element or isotope distribution analysis. See Figure 2.5.

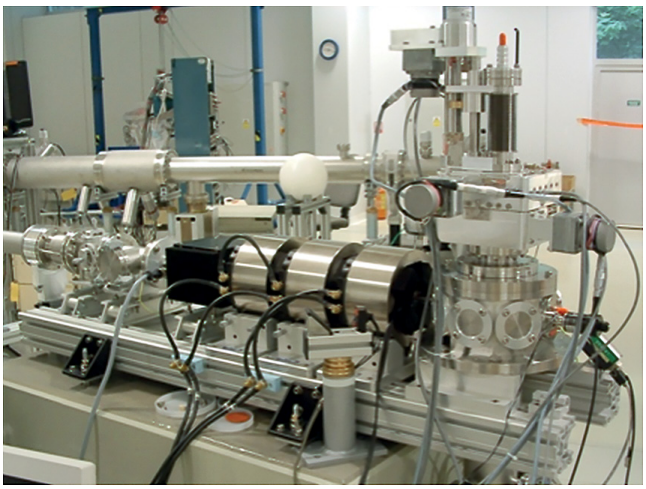

**Figure 2.4:** Microbeam arrangement at the Center of Accelerators and Nuclear Analytical Methods (NPI CAS), Czech Republic, showing the vacuum chamber for the specimen on the right and a triplet of magnetic quadrupole lenses for focusing the beam to sizes of a few micrometers.

With protons or heavy ions, the mean free path between ionising events is generally much shorter than the specimen thickness and multiple inelastic collisions occur. The energy-loss spectrum becomes a measure of specimen thickness rather than elemental content. In proton microprobe (PMP), with a typical energy of 3 MeV, the proton range is some tens of micrometers and the mean free path between inelastic collisions is under 100 nm.

In bright-field transmission imaging, the transmitted beam runs directly into a detector and the beam current is restricted to about $10^4$ particles $s^{-1}$. PMP gives a spatial resolution for microanalysis of about 1 μm, with 100 pA beams of protons or α-particles. Some effects must be taken into account, such as the charging of insulating components and the removal of some components by sputtering, which prevents repeated investigations. Image contrast may also arise from chemical or topographic rather than isotopic differences.

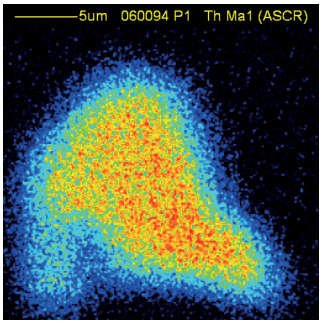


**Figure 2.5:** 2D microbeam mapping of the elemental composition of an inclusion in a granitic rock, obtained by scanning the microbeam. The colour indicates the concentration of the element studied with the highest concentration depicted by the red and yellow colours.

### EXTERNAL BEAMS

In practice materials or artefacts are often obtained which cannot be placed in a vacuum chamber because of their large size or because of volatile components. Such samples can be analysed using an external ion beam, extracted from an evacuated beam line into air through a thin window. This typically reduces the beam energy by 20-200 keV.

The window materials are either thin metal foils, such as aluminium or tungsten, or strong plastic materials like kapton or $Si_3N_4$, which is now widely used. This material typically has a very low thickness, about 0.1 μm, to minimise the energy loss and angular straggling of the external beam. In a standard arrangement the beam spot at the target is a millimetre or less in diameter if the beam is shaped by slits, but may be as low as 10 to 30 μm if the beam is focused using magnetic optics.

Targets are normally mounted on a computer-controlled x-y-z placeholder. Practically all arrangements now allow the scanning mode of measurement that produces concentration maps. The target is encircled by an array of detectors: normally at least two X-ray detectors are used: a thin window detector for soft X-rays and a detector with a large solid angle, but equipped with an additional absorber, for hard X-rays. The target region may be flushed with helium to reduce X-ray absorption and X-ray background arising from interaction of the ion beam with Ar in the air.

In recent measurement configurations, X-ray Si(Li) detectors are replaced by arrays of SDD (silicon-drift detector) diodes and induced γ-rays are measured by HPGe or scintillating (NaI-Tl) detectors. Analyses can also be carried out at external beam RBS and ERDA and, for this purpose, flushing with helium is necessary. Some other types of spectroscopy are installed at some facilities, such as ion-induced optical luminescence where optical spectra can reveal information on chemical bonding.

## 2.3. APPLICATIONS OF IBA

The application of atomic and nuclear techniques to the study of archaeological objects gives the historian or the archaeologist *materials* information that helps understanding life during ancient times. This knowledge is necessary to test the authenticity and provenance of artefacts and to prepare and carry out restorations. These objectives are common to the large community of people working in archaeometry, *i.e. the application of science to art and archaeology*. In the case of investigating metallic artefacts, the domain is called *archaeometallurgy*. For these research activities a multidisciplinary community of action is essential.

IBA techniques are based on relatively simple, well-known physical processes and the extraction of the required information from the measured spectra is reasonably straight-forward. IBA measurements and data evaluation can also be performed in a relatively short time. With a single experimental facility, simultaneous analyses using various IBA methods can be accomplished and more complex analytical information easily obtained. This work brings together physicists, chemists, archaeologists, numismatists, historians, geologists and conservators from different laboratories, institutes and museums.

### 2.3.1. METALS

Archaeological metals are efficiently studied by ion-beam methods; however, one has to consider that the range of MeV particles in metal is typically 10-30 μm, which renders the techniques such as PIXE surface-sensitive only. As archaeological metals are normally covered by oxides up to a millimeter thick, these have to be removed in order to get information on the bulk composition. Surface polishing is often not permitted by museum curators, though they may consent to it if the collected analytical information is valuable. Such corrosion problems are virtually absent with noble metals, though one has to be aware that some metal enrichment at the surface may occur due to selective oxidation or leaching of less noble metals.

As an illustrative application of metal analysis we show a study of Roman brass [27]. Brass, an alloy of copper and zinc, appeared relatively late among the set of historical alloys. The problem of alloying brass is a low evaporation temperature of zinc; zinc may evaporate before the copper melts. Brass was first produced only occasionally by melting together copper and zinc ores, until the invention of the so-called cementation technique. This procedure relies on the simultaneous reduction of zinc ores in the presence of copper in a sealed container which enables simultaneous diffusion of zinc into copper. The maximum percentage of zinc in cementation-produced brass is 28% [28]. Brass coins appeared among the Hellenistic Greeks around 100 BC.

Polished brass with its gold-like lustre was an attractive material for Roman military equipment, such as brooches and the fitments of sword sheaths. The onset of the application of brass in the Eastern Alpine region was determined from the composition of brooches [29].

Brooch types change frequently according to fashion and the occurrence of particular types is well dated archaeologically. This study showed that brass appeared in some examples of the brooch type A*lmgren 65*, while later *Alesia* type brooches were generally made of brass. This puts the first use of brass at around 60 BC. This dating

is considerably earlier than the Augustan money reform of 23 BC, which was traditionally considered as the onset of brass use, largely based on the introduction of the brass coin types *dupondii* and *sestertii*. The results of the brooch analysis showed that the use of brass started about 40 years earlier.

The use of brass further implies complex relations between the Romans and their barbaric neighbours. Several swords found at the border of the Roman Empire were made in Late Iron Age (*La Tène*) style, though their material is brass, *i.e.* typically Roman. Measurements were made using an in-air proton beam in order to allow the analysis of large objects and the samples were prepared for measurement by gently polishing small areas of the material [30].

The archaeologist J. Istenič explains the disparity between the style and use of the material as a result of involved international relations: the objects were produced in Roman workshops and intended as gifts for noblemen that lived on the border of Roman Empire and had important contact with the Romans, yet their archaic taste was still bound to the Late Iron Age forms [31].

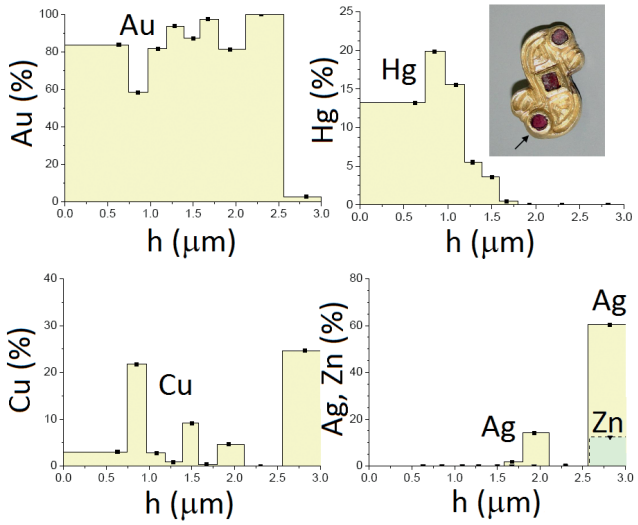


**Figure 2.6:** Au, Hg, Cu, Ag and Zn concentration profiles of the gilded layer on a Late Antique brooch obtained by differential PIXE; h is the distance from the surface [33].

The second example of metal analysis demonstrates identification of gilding techniques. The objects studied were from the Late Antiquity, which favoured gilded silver or bronze jewellery with inlaid garnets. The methods applied were differential PIXE and Rutherford spectroscopy with an in-air proton beam [32,33]. Figure 2.6 shows the measured Au, Hg, Cu and Ag concentration depth profiles of a Late Antique brooch [33].

The measurements were made at nine impact energies ranging from 2.78 MeV to 740 keV. The gold layer is found to be about 2.5 μm thick, but the gold is not pure: throughout the profile it is mixed with mercury, which undoubtedly reveals that a fire gilding or amalgamation procedure was used. For this technique, a paste of gold amalgam is applied to the object surface. The object is then heated until the mercury evaporates and a solid gold layer forms at the object surface. The evaporation of mercury is never complete; the gold layer typically contains up to 15% mercury, which then remains as a clear indication of the technique.

Gold and mercury layers may also be identified by RBS; however, the mass resolution of the experiment does not allow clear separation of the weak mercury and strong gold signals. The presence of mercury has to be confirmed using X-ray spectra. The codes for concentration profile de-convolution are still being developed, and the combined use of X-ray and backscattered particle spectra seems to be the most efficient [34].

Ion beam techniques can also be used for the identification of the surface layer of tin and silver, though the thickness of silver may exceed the range of particles at the highest impact energy, thus giving an impression that the object is made of solid silver.

### 2.3.2. GLASS

Glass is an artificial inorganic compound composed of many elements. Their relationship varies significantly over historic periods, so the analysis of glass may provide valuable historical information about the sources of raw materials and their transport routes.

Glass is generally composed of three main components: siliceous matrix, alkaline flux that lowers the melting point and alkaline earth oxides required for chemical stability. As the agents used for glass production are not chemically pure, but contain significant amounts of metal impurities, notably iron, common glass is usually coloured. The influence of iron is neutralised by decolourants, which turn valence-two iron into its three-valence form. The use of decolourants is also historically dependent.

Glass may further be coloured, yet the amounts of required colourants are so small (at the percentage level or below) that they hardly change the bulk composition.

The multi-element composition of glass is challenging for different analytical methods. The advantage of ion-beam methods is the non-destructive nature of the investigation: whole objects may be analysed at particular points, without sampling. Archaeological objects may be covered by a layer of oxides, which should be removed before measurement. Surface leaching of alkaline elements may occur and an assessment of this effect has to be made. Glass may be regarded as a mixture of metal oxides, so the lightest element to be detected is sodium.

In order to separate sodium and magnesium using the PIXE analytical method, the measurement has to be performed in vacuum or in a helium atmosphere using a thin window X-ray detector. Alternatively, low Z elements are determined by PIGE, which exploits detection of γ-rays

induced by inelastic proton collisions. Sodium lines are intensely produced in deeper regions of the target (below 10 μm), so detection of bulk sodium is straightforward. Detection of magnesium is less favourable, as the production rate of magnesium lines is lower, yet the most intense γ-ray at 585 keV lies very close to the 583 keV γ-ray, which exists in natural background radiation. With careful measurement, a detection limit of 0.2 % magnesium can be reached, which is just sufficient for the glass of the Roman period.

Glass also contains important trace elements around strontium and zirconium, which are important indicators of raw material provenance. The sensitivity of ion-beam methods to these elements and to the rare earth elements is much lower than achievable by several chemical methods, yet useful data may be obtained from hard X-ray PIXE spectra.

**Figure 2.7:** Chunk of glass discovered close to the Roman settlement Nauportus, presently Vrhnika in Slovenia [40]. Analysis based on the PIXE-PIGE method demonstrated that the material was natron-type glass characterised by sub- percent concentrations of MgO and $K_2O$. This indicates that the material represents primary Roman raw glass intended for further reworking in secondary workshops.

High energy X-rays are detected by a detector with a large solid angle, simultaneously suppressing the intense low energy X-rays with an absorber. Recent glass studies [35] deduce important information from the isotopic ratios $^{87}Sr/^{86}Sr$ and $^{143}Nd/^{144}Nd$; this type of measurement is unfortunately not obtained by ion-beam methods.

Historic glasses are dominated by the choice of alkalis which are obtained from the ash of plants or from mineral deposits. The latter category involves glass produced with natron, a dried sediment from Egyptian lakes. Natron-based glassmaking developed in the area of present Egypt, Palestine and Syria and dominated glassmaking in the Greek, Roman and post-Roman world during the long period from 800 BC to 800 AD. Glass produced in the second millennium BC in Bronze Age Egypt and Mesopotamia was made of ash of halophytic plants of either maritime or dessert origin. The same species of plants were also used during the transition period between 800 and 1200 AD and represented the basis of Venetian glassmaking.

In central and northern Europe, beech ash was used instead, which produced potassium-rich forest glass. From the analytical viewpoint, it is relatively easy to distinguish between different types of glass. Sodium glasses are distinguished according to the level of magnesium and potassium impurities: natron is generally much purer than ash of halophytic plants. The concentration of sodium is small compared to potassium in forest glass. Ash was subject to different purification procedures. The most rigorous was making potash through precipitation, which can be recognised through the absence of soluble metal oxides in the finished glass objects.

The most important question regarding Roman glass is its primary production site. According to Pliny, glass was produced in the Levant area, but also in Italy, southern France and Spain. Archaeological and analytical data show that during the late Antiquity, raw glass was produced entirely in the Levant area and distributed to secondary workshops elsewhere in the Empire in the form of glass chunks. New studies based on isotope distribution suggest that raw glass was made in the western and eastern part of the Mediterranean during the Imperial period ($1^{st}$ - $4^{th}$ c. AD), but production centred in the eastern part in the late Antiquity [35].

Measurements performed at Ljubljana involved Greek glass from Apollonia Pontica [36] and Roman glass from Albania [37], Bulgaria [38] and Serbia [39]. In the latter case we identified a glass chunk (Figure 2.7) made of natron-type glass [40] and measured glass from a hilltop post-Roman settlement [41].

The results show multiple sources of raw materials for the Albanian glass which is consistent with the model of dispersed raw glass production. Glass in the later periods becomes less pure, mainly due to repeated recycling. New glass types came into use in late Antiquity, showing established commercial routes across the Mediterranean and Italy.

The first items to reveal new glass technology around 800 AD were glass beads, produced in the Islamic East. As commercial items they spread much faster than the raw glass. A systematic study of glass beads excavated in Slavic graves in Slovenia [42] showed two significant groups: beads made of natron-type glass according to the Roman tradition and beads made of the ash of halophytic plants (Figure 2.8). The occurrence of the latter is important for dating: certain graves in Slovenia were dated to the $7^{th}$ and $8^{th}$ c. AD in early studies, but now have to be dated later, to the first half of the $9^{th}$ c. AD because of the presence of glass beads made from plant ash. This dating is consistent with the dating of the Köttlach culture in central Europe.

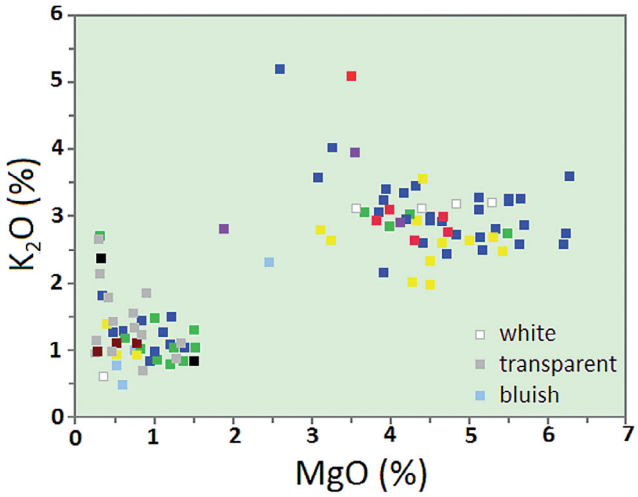


**Figure 2.8:** Concentrations of potassium and magnesium oxides in early medieval glass beads excavated from graves in Slovenia, determined by a combined PIXE-PIGE method [42]. Glass made from Egyptian natron (lower left, with low magnesium and potassium values) and glass made from ash of halophytic plants (upper right, high magnesium and potassium) form two distinct groups. The latter type of glass spread after 800 AD. This information can be used to date the graves.

Production of glass made from the ash of halophytic plants, collected at various Mediterranean coastal locations, peaked in the period starting roughly in the 13th c. and ending in the 17th c. The main producer was Venice.

Glass from Venice is known as Venetian glass. Glass produced in the same manner, but outside Venice, is labelled as glass *à façon de Venise*. For historical sites that show abundant glass finds it is important to know if they produced glass locally or if they imported it from Venice. The same question arises regarding Ljubljana, where about 800 glass fragments are kept in the National Museum and local production of glass is documented in historical records. The analysis using the PIXE/PIGE method of more than 300 specimens showed two distinct groups [43].

The comparison with other glasses from Western Europe and Italy showed that the two groups are universal and imply two different ash sources [44,45]. One is undoubtedly Venetian, but interpretations for the other group differ: though it also contains samples of Venetian origin, it may also indicate glass *à façon de Venise* [45]. However, as the same glass type was also identified among the much earlier medieval glass beads and glass around the Aral Sea [46], this type of glass may only suggest a specific ash source from a certain, presently unidentified plant. Further development of glass technology in Venice resulted in a much finer and transparent *cristallo* glass. In the 17th c. *cristallo* was also produced outside Venice, for example in Antwerp.

The switch to the new technology was nicely observed among the glass of the Albanian city of Lezha: besides the two groups of common Venetian glass, a distinct group was identified that was made of purer silica and alkalis purified by precipitation. The glass was further discoloured by arsenic, which replaced manganese in the former Venetian glass [47].

Individual properties of particular glass producers may also be identified for the glass of the late 19th and early 20th c. A study on uranium-pigmented and red glass kept at the National Museum of Slovenia showed that the glasses were produced in three different places: one was very likely located in the present Czech Republic, while the other two were in Slovenia, one being identical with a present day glass factory in Hrastnik [48].

### 2.3.3. CERAMICS

Archaeological ceramics have a coarse-grained structure which renders analysis by millimetre beams unreliable, unless the samples are finely ground and homogenised. The advantage of non-destructive ion-beam methods is thus lost, and the powder obtained can be equally well analysed by wet chemical methods or in the form of pellets that can be analysed by a variety of methods. Using a particle microbeam on the cut and polished surface it is possible to identify particular mineral species. On the other hand, bulk analysis can be successful on objects made of cream-coloured ceramics [49]. The material is sufficiently homogeneous that measurements in selected, glaze-free, areas can give representative results.

Cream-coloured ceramics were invented in England in the 18th c. as an inexpensive substitute for porcelain. Northern Italy (then part of the Austrian empire) soon

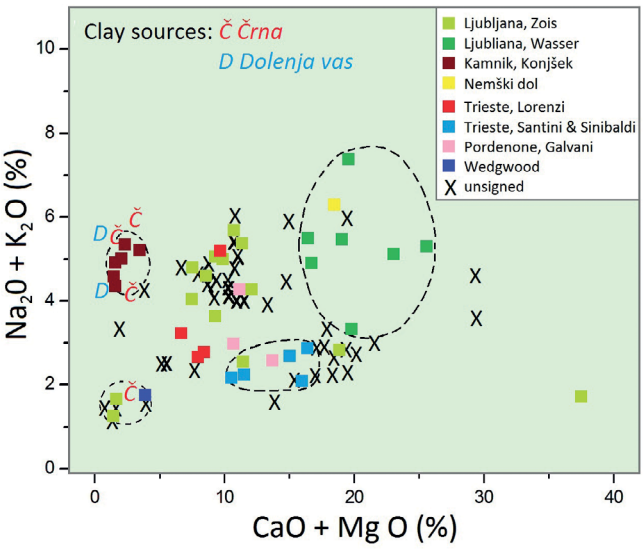


**Figure 2.9:** Compositional groups of cream coloured ceramics produced during the 19th c. in the present day territories of Northern Italy and Slovenia, determined by PIXE-PIGE analysis. Items corresponding to two separate sources of white clay extracted in Slovenia both have low CaO + MgO concentrations.

followed as a significant production centre, as did the neighbouring countries of present day Slovenia where two deposits of white clay were discovered. The composition of selected objects from the National Museum of Slovenia was measured by the combined PIXE-PIGE method following the procedures developed for glass analysis.

A statistical analysis based on principal components was able to distinguish particular producers, but was not able to distinguish between the two clay sources (*Č. Črna* and *D. Dolenja vas* in Figure 2.9). The differences between the producers arose from mixing the primary batch with different minerals, notably limestone. It was possible to observe that one producer (S. Zois - lime green) largely experimented with different mixtures, as documented in his notebooks.

### 2.3.4. PRECIOUS STONES

Precious and semi-precious stones were popularly worn in Antiquity: emeralds by Romans and garnets by their barbaric successors. Analysis of precious stones is similar to the analysis of glass as their composition can be interpreted as a combination of metal oxides. PIGE is used for light elements and PIXE for medium and heavy elements. Emeralds contain a known fraction of beryllium which can be measured either directly or taken into account numerically for the calculation of matrix effects.

The provenance sites of precious stones are of particular interest as they indicate the extension of commercial routes first established by the Romans. However, the determination of emerald sources is not unambiguous [50] and additional mineralogical and gemmological investigations have to be carried out.

For example, the fluid channels in a set of emeralds excavated in a Roman grave from Slovenia point to a source in Egypt, while emeralds from another grave may be traced to Afghanistan [51]. Interestingly, the emeralds were not from a nearby source at Habachtal in Austria.

Elemental analysis proved useful for provenance studies of garnets. The majority of garnets in Europe came from India and Sri Lanka. There was a disruption of transport routes by the end of the 6$^{th}$ c. AD due to the Sassanid seizure of the Arabian peninsula. Garnets from Bohemia (present day Czech Republic) and Portugal were subsequently used in the Merovingian kingdom [52-55]. Interestingly, Bohemian garnets are absent in the territory of present day Slovenia despite the proximity of the sites.

The reason is very likely to lie in the incursions of Avars and Slavs who did not follow the fashion of their Germanic predecessors [55]. But also in the West, the low quality of new stones heralded a decline in garnet embroidered jewellery.

### 2.3.5. PIGMENTS AND PAINTINGS

In-air particle beams are an ideal tool for the investigation of paintings and the identification of metal-based pigments. Low intensity beams and short exposure times cause no radiation damage to pigment layers. A brief measurement can identify the type of pigment, which may have a historic context, and can discover later repairs and curator treatments. For example, a very short measurement can distinguish between lead, zinc or titanium white; the third is a pigment introduced in the 20$^{th}$ c. The measurements are particularly interesting for 19$^{th}$ c. paintings, since the rapidly developing chemical industry of the period introduced many new synthetic pigments.

Though pigment identification can be equally well established by a much cheaper X-ray apparatus, the main advantage of ion beam methods is a combined application of different methods, including differential measurements. Performing a series of measurements in the same spot, it is possible to determine the composition of particular paint layers. For example, using differential PIXE it is possible to determine the composition of the layer with the signature of the painter [56].

### 2.3.6. PAPER

Records on paper preserve a crucial part of human cultural heritage. Historical archives contain many hand-written documents with iron-gall ink on an acid paper. With time, the ink acts corrosively on the paper and virtually destroys it. Ion beam methods have been successfully applied to detect iron-based inks and can also provide the concentrations of other heavy elements such as copper and zinc. Though the methods cannot be used for the precise identification of the chemical state of these elements, they are efficient in the fast detection of iron-gall inks [57]. They can also distinguish between particular inks and thus between particular writers.

PIXE on graphic works can provide other important information: *e.g.* this technique can identify the types of pencils used (graphite, lead or silver) or pigments, such as lapis lazuli, in hand-painted incunabula. It is also possible to identify printing inks and a number of printing offices.

### 2.3.7. CHINESE MING POTTERY (FROM ANGKOR THOM)

The purpose of the investigation was to assess the possible origin of Chinese pottery shards (presumably dating to the Ming dynasty) found in excavated material from an ancient pool at the royal palace grounds of Angkor Thom. As the former imperial city was abandoned shortly after its sacking by the Thai armed expedition in 1431 AD it seems most probable that the artefacts found on the grounds had been imported by the Royal court while still at Angkor Thom, that is some time before that date.

The study aimed to separately analyse the composition of the glaze and painted sections containing cobalt.

A further aim was to find the possible origin of the kilns in China where the shards found were manufactured. This would be done by comparing the composition of the cobalt with reported measurements of elemental composition made with PIXE on shards found at various kiln locations in China.

The shards were sliced into thin sections and examined with a microscope coupled to a camera to allow identification of the blue pigment depositions and the glaze. The samples were placed in aluminium holders and irradiated with a proton beam of about 150 pA, focused to a 1 μm spot using an Oxford triplet of magnetic quadrupole magnets. The proton beam energy of the Tandetron accelerator at the Řež Microprobe Facility, was varied between 2 and 3 MeV according to the molecular weight of the elements studied in a particular experimental session.

The X-ray emissions from irradiated shard slices were recorded using an 80 $mm^2$ Si(Li) detector. Furthermore, the RBS spectra were measured simultaneously using a PIPS detector. The diameter of the focused beam was equivalent to 9 pixels of the resulting 2D-maps, which showed the concentration of each particular element. Up to 20 elements were determined during each measurement.

The maps of individual elements were constructed from their emission spectra. The advantage of the measurements reported here over those reported previously was their superior spatial resolution which enabled pertinent sites to be targeted, reducing the partial volume effects associated with measurements using wider beams.

The 2D maps of elemental composition revealed a high calcium content, greater than 10%, in the pottery glaze. This rather high concentration is compatible with values for calcium compositions reported for Chinese pottery of the Ming dynasty, presumably produced prior to 1431 AD.

The cobalt pigment sections showed high concentrations of arsenic. Arsenic is a major constituent of asbolite that was presumably the source of the pigment imported during the Ming dynasty from Persia. Cluster analysis of the elemental compositions determined for the glazes on numerous shards showed the feasibility of ascertaining their provenance. From the elemental composition of the cobalt pigment and glazes, it appears that the pigment was most likely imported from Persia and that the shards analysed were manufactured in kilns at two distinct locations in China [58].

### 2.3.8 TYCHO BRAHE - WAS HE MURDERED OR WAS HE NOT?

World-renowned Renaissance astronomer Tycho Brahe died on 24 October 1601, after 11 days of sudden illness. Several conspiracy theories, suggesting mercury poisoning, were aired shortly after his death. In 2010, Brahe's grave in Prague was reopened and samples of his bones, hair, teeth and textiles were procured and analysed. The hairs with identifiable roots (Figure 2.10.) were cut into sections about 5 mm long and washed using the IAEA recommended procedure [59].

Sectioned samples from 20 to 25 individual hairs weighing 200 to 300 mg were sealed in pre-cleaned high-purity quartz ampoules and irradiated for 20 hours at the Czech Academy of Sciences LVR-15 nuclear reactor in Řež at a thermal neutron fluence rate of $3 \times 10^{13}$ $cm^{-2}s^{-1}$. The $^{203}Hg$ produced was separated after 2 to 3 weeks decay using an RNAA procedure (see chapter 3) [59] based on Hg extraction with 0.01 mol $L^{-1}$ Ni diethyl dithiocarbamate ($Ni(DDC)_2$) and measured by high-resolution γ-spectrometry. Unsectioned hair samples were also analysed by μ-PIXE, using a Tandetron 4130 MC accelerator with a 2.6 MeV proton beam focused to a diameter of 1.5 mm. Multiple scans were performed over 500 mm sections of hair at a 0.1 nA beam current for 1 to 3 hours.

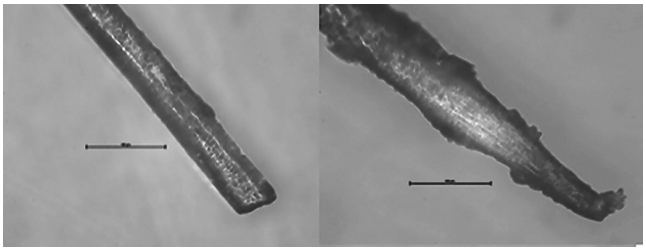

**Figure 2.10:** The hair tip and root from a sample of Tycho Brahe's hair. The inserted scale is 100 μm.

Figure 2.11 shows excellent agreement between the RNAA and μ-PIXE results for one analysed hair sample and compares the values found with the median and range of Hg content in the contemporary unexposed population. Hair provides a lasting record of exposure to trace metals over the last few months of life. The hair samples analysed in this study reflect the Hg intake over approximately the last 2 months prior to the death of Tycho Brahe, assuming the most frequently cited hair growth rate of 10 mm per month [60].

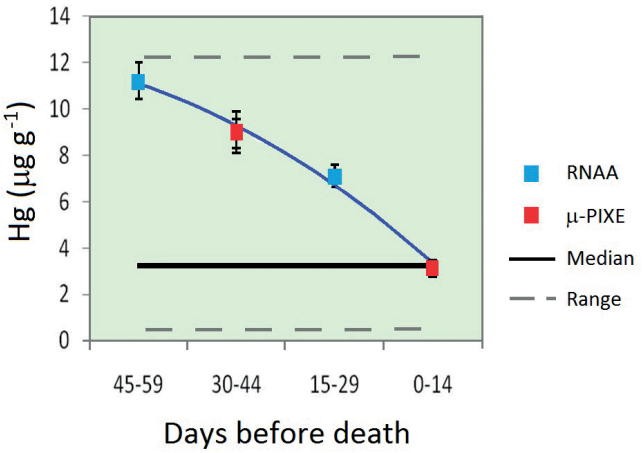


**Figure 2.11:** Time dependence of the Hg content in one sample of Tycho Brahe´s hair measured using RNAA and μ-PIXE techniques, compared to the median (black solid line) and range (grey dotted lines) of Hg content in contemporary unexposed populations.

The highest Hg values found are slightly above the median of *normal* values, and well within the normal range. Their reduction towards Brahe's death, suggests that he was not exposed to excessive Hg doses shortly before his death (no acute poisoning).

Analysis of Brahe´s bones also revealed no long-term exposure to Hg (no chronic poisoning). Thus the analyses carried out prove that the famous astronomer was not poisoned by Hg and a murder scenario has become a much more remote possibility than previously thought.

### 2.3.9. ORIGINS OF THE SARMIZEGETUSA GOLD BRACELETS

It is already well-known that trace elements are more significant for determining the provenance of archaeological artefacts than the main components for gold, silver, obsidian or copper-bronze items. Because a high sensitivity elemental analysis of valuable museum objects is quite difficult – especially expensive due to transport and security problems – an adequate solution is to complete *in-situ* XRF analysis in museums. Micro samples are taken and studied using advanced micro-spectrometric X-ray methods. The micro-PIXE technique, which is sensitive at a level of a few ppm and has excellent lateral resolution, is capable of micro-inclusion detection and is one of the best available methods of providing information on the provenance of archaeological artefacts.

**Figure 2.12:** Dacian spiral gold armbands studied by XRF analytical methods.

For the authentication of ancient gold artefacts (jewellery and coins) found on Romanian territory, the most likely use of unrefined Transylvanian gold must be considered.

In ancient times, and up to the Middle Ages, the most important source of gold was placer deposits. Alluvial gold is derived from weathered rocks containing veins of gold deposits. Gold is highly resistant to weathering; its particles are washed down mountains along with weathered rocks, and are subsequently deposited in the sand and gravel of rivers.

Naturally occurring gold contains several impurities, most notably silver and, in a much smaller proportion, copper. During the weathering and transport of gold particles, silver and copper are more susceptible to dissolution or leaching, depending on the pH value of the environment. Consequently the overall silver and copper content of alluvial gold is somewhat less than the content of the vein gold from which it is derived.

A relevant demonstration of the use of alluvial gold in prehistoric times in Transylvania – one of the richest gold producing regions in Antiquity – is a series of complex studies performed between 2007 and 2012 on Dacian gold artefacts, including 13 spiral gold armbands, see figure 2.12. (These artefacts were discovered illegally in the Sarmizegetusa area by treasure hunters using metal detectors.) The compositional analysis of the Au-Ag-Cu content of the armbands confirmed they were made of native Transylvanian gold. The presence of tin indicated an alluvial deposit. Some antimony, which is one of the main fingerprints of a primary Transylvanian gold vein, was also observed [61-64].

### 2.3.10. PROVENANCE OF LAPIS LAZULI

Lapis lazuli is a semi-precious blue stone which has been used widely since antiquity for many different purposes. However, information regarding the quarries used by different civilisations to extract the mineral and information about its trade in ancient times remains scarce.

Historical sources of lapis lazuli are located in inaccessible places, such as the Afghan and Pamir Mountains and stones were transported for thousands of kilometres. Unfortunately, these trade routes are largely incomplete and unknown. Only a few sources exist in the world because of the restricted compositional and physical constraints in which lapis lazuli can form [65]. Therefore assigning sources of raw material to man-made objects can help historians and archaeologists reconstruct ancient trade routes.

A systematic study (see Figure 2.13) of this fascinating stone compared the physico-chemical properties of rocks from four different sources (Afghanistan, Tajikistan, the Lake Baikal region and Chile) [66-72]. Many analysed lapis lazuli rocks and objects come from the collections of the Museo di Storia Naturale (University of Florence, Italy). About fifty pieces of lapis lazuli are conserved in this collection. Half of these are blocks of rock, which are rough or partially polished, and the other half consist of carved objects of exquisite workmanship and fragments or whole tesserae for inlays.

Recently other groups have started to study lapis lazuli, both as rock and as ultramarine blue pigment, for provenance identification, using different approaches and obtaining interesting results [73-80].

Due to the paragenetic mineralogical heterogeneity of lapis lazuli, the single mineral phases were analysed to search for markers useful for a provenance study. Since

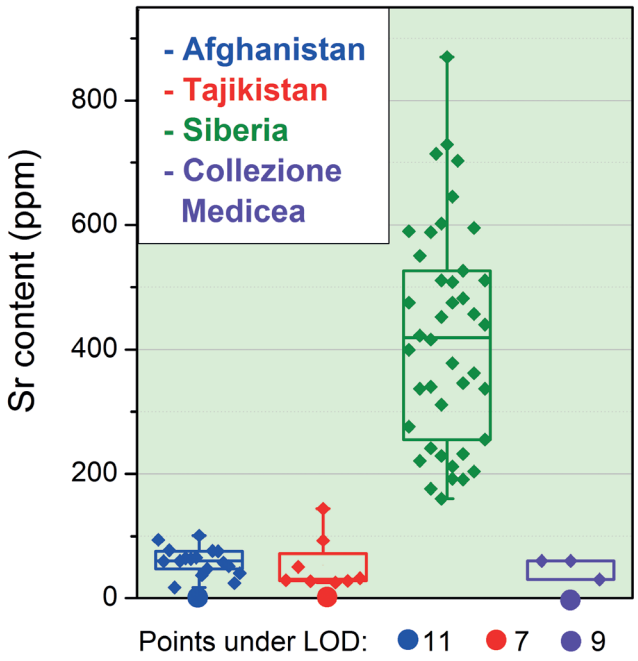


**Figure 2.13:** Sr content in diopside minerals from various sources. The boxes contain the central 50% of measurements, while the vertical bars indicate the full range of the measured data. The horizontal lines in the boxes divide the data in two identically sized groups. The large dots at zero content indicate points with Sr content below the detection limit.

crystal dimensions vary from a few microns to hundreds of microns, high spatial resolution techniques are mandatory. IBA techniques with an external proton microprobe were used. External IBA allows for non-invasive, multi-technique (PIXE, PIGE, and ion beam induced luminescence IBIL) studies of objects of almost any shape and dimension; see for example Figure 2.14.

The study focused on identifying markers, such as the presence (or absence) of a specific mineral phase in the stone, the concentration of trace elements in a mineral or the luminescence features of a particular crystal, in order to identify the provenance of the stone.

A multi-technique approach, including optical microscopy, SEM-EDX, cathodo-luminescence, Raman spectroscopy and in-vacuum IBA is used to identify markers in the analysis of rocks from a particular provenance. A non-invasive IBA analysis is performed on the artworks containing lapis lazuli and the previously discovered markers are used to identify the origin of the stone used.

Some of the markers identified on stones have been successfully used in the study of six precious artworks from the *Collezione Medicea* (see Figure 2.14) made in lapis lazuli [73].

The identification of the regions to be analysed was carried out using a broad beam ion luminescence microscopy setup [81]. This gave a preliminary indication of the distribution of different mineralogical phases and allowed the biggest and most homogeneous crystals to be selected.

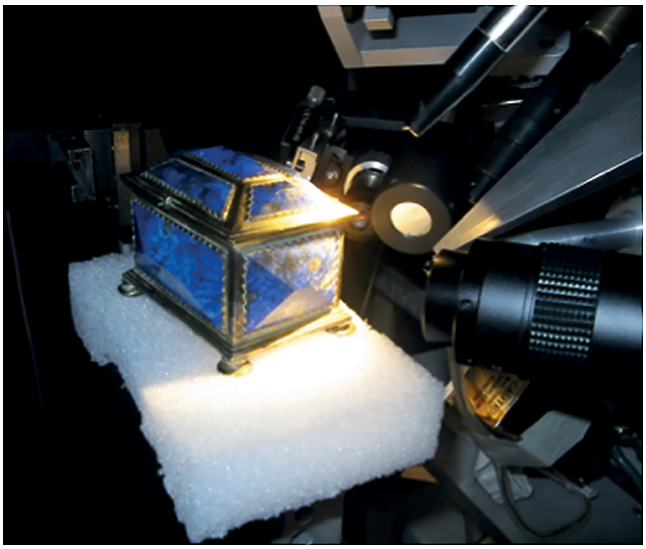

**Figure 2.14:** An artwork from the *Collezione Medicea* photographed during an external microbeam IBA analysis carried out at INFN-LABEC, Florence.

After this preliminary selection, ion microbeam analyses (μ-IBIL and μ-PIXE) were performed on selected crystals. Ion luminescence allowed a Chilean origin to be excluded because of the absence of wollastonite, a mineralogical phase typical of Chilean provenance. Wollastonite is characterised by a particular luminescence pattern which was not observed in the IBIL measurements on the artworks.

The rocks from the three Asian provenances are all characterised by the presence of diopside, a luminescent mineralogical phase commonly present in lapis lazuli. The content of trace elements inside this phase in all the artworks studied was measured using μ-PIXE and compared to the rock database.

Among the detected elements, Sr has the sharpest capability to discriminate between different provenances: a quantity higher than 150 ppm has only been detected in Siberian samples. In the *Collezione Medicea* artworks, the Sr content is always below 100 ppm, so the Siberian provenance can be excluded (Figure 2.13.).

The amount of other trace elements (titanium, vanadium, chromium) in this phase, combined with some luminescence features, allowed an Afghan origin to be ascribed to the material used for five of the six artworks studied. For the sixth artwork a Tajikistan provenance cannot be excluded and a further analysis, *e.g.* checking markers related to other phases such as pyrite, is needed to confirm or reject an attribution of origin to the Afghan provenance.

### 2.3.11. *LA MADONNA DEI FUSI*, BY LEONARDO DA VINCI

The depth sequence of elements in paintings can be obtained using differential PIXE (d-PIXE). PIXE measurements are made at the same place with a range of beam energies. The sequence of layers can be inferred, at a semi-quantitative level, by comparing the X-ray spectra collected at different incident beam energies.

The interpretation of d-PIXE data is complicated by several factors. For example, the number of layers and their thickness is unknown, so that the choice of the beam energies to separate the contributions from the various layers is not straightforward. Moreover the particle energy distribution becomes larger with depth, so that a clear-cut discrimination of the layers cannot be readily achieved.

A PIXE/d-PIXE/PIGE study was performed on the famous painting by Leonardo da Vinci the *Madonna dei fusi* (ex-Redford version) [82,83], shown in Figures 2.15 and 2.16. This study aimed to discover the peculiar features of his painting technique. Particular care was devoted to the characterisation of the protective varnish and the blue pigments, in both the original and the restored parts.

Very safe experimental conditions were adopted, in order to avoid any risk of damage: the 2.7 MeV proton beam was extracted into a He atmosphere, with a beam current of some tens of pA in measurements which lasted a few hundred seconds. The beam was about 1 mm in diameter.

The varnish covering the *Madonna dei fusi* made it difficult to detect light elements which are characterised by low energy X-rays. The lower the energy, the higher the X-ray absorption. In addition, the varnish contained many trace elements, detected by PIXE measurements, which constituted a source of "contamination" for the pigment identification.

The varnish thickness was estimated by calculating the range of protons in organic material at the highest beam energy where the contributions from the pigment layer were not yet visible. Values ranged from 30 to 50 μm.

The first step of the study was the determination of the varnish composition and thickness. As the beam energy is reduced to the point where the contribution to the spectrum from elements characteristic of the paint layers disappears, it can be assumed that the protons stop in the overlying varnish.

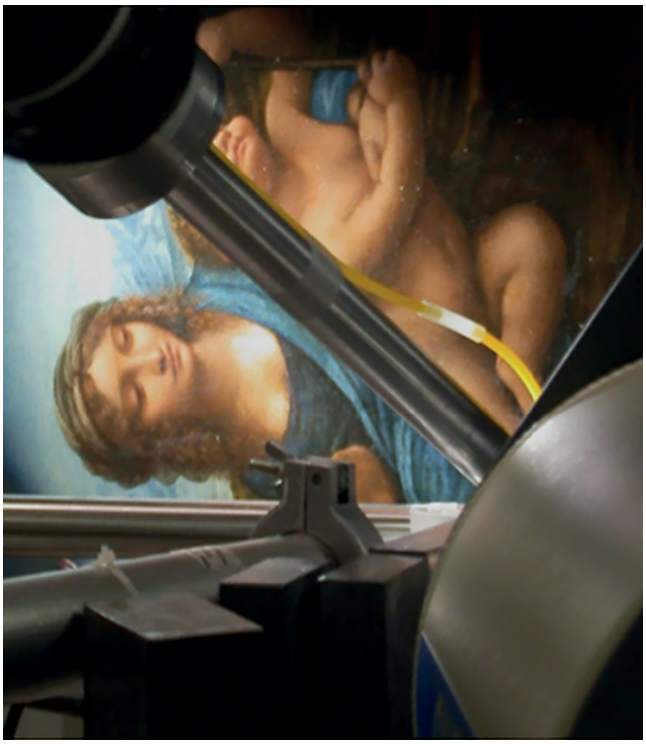

**Figure 2.15:** *The Madonna dei fusi* at the PIXE-PIGE set-up in Florence.

**Figure 2.16:** The *Madonna dei fusi* during the measurements. The protective varnish is evidenced by the *mirror effect*.

In the second phase, we carried out a PIXE analysis of some of the blue areas. Large quantities of Zn and Co (the latter associated with relevant amounts of Al) were detected and were attributed to the presence of zinc white and cobalt blue (cobalt aluminate). These pigments have been used only since the beginning of the 19th c. and consequently those areas were identified as restorations.

When bombarding other blue areas, only a large amount of Pb was found, clearly associated with lead white; no elements characterising a blue pigment were detected by PIXE. The use of lapis lazuli for these blue zones could only be hypothesised: the use of the most probable period-compatible alternative blue pigment (azurite, copper carbonate) was excluded, since Cu X-rays would have been detected even in the presence of the varnish. Due to their rather high energy (about 8 keV), Cu X-rays have a good transmission through some tens of microns of organic material.

A direct demonstration of the use of lapis lazuli is typically achieved through the detection of Na X-rays. Na is the fingerprint of lazurite, the mineral responsible for the beautiful blue colour of the stone. Unfortunately, the presence of the varnish over the pigments makes it difficult, or even impossible, to detect light elements: the lighter the element, the lower the energy of the produced X-rays and the higher their absorption in the varnish. This is especially true for Na, the lightest element detectable by external PIXE. For instance, 10 μm of organic varnish (a value which can be considered a lower limit for the thickness of a varnish) absorbs more than 97% of the 1.041 keV Na X-rays.

The highest-Z element of lazurite, S, which is less affected by absorption, is hard to identify in the presence of a large amount of Pb (as in this case, where the blue pigment was mixed with lead white), as the $Pb_{M\alpha}$ lines ($E_{M\alpha}$=2.345 keV) largely overlap the $S_{K\alpha}$ ($E_{K\alpha}$=2.308 keV) lines.

Finally, detecting Al and Si by PIXE cannot be considered a fingerprint of the presence of lapis lazuli, since these elements are found in many other pigments which may be added to the paint layer *e.g.* to modify the chromatic shade.

The PIGE method was successfully applied to the study of the blue pigment of *la Madonna dei fusi*. All the spectra acquired in the original areas showed a strong peak at 441 keV, while those corresponding to the restored zones showed no peak at all in the same energy interval. This directly demonstrated Leonardo's use of the lapis lazuli pigment, notwithstanding the overlying protective varnish. To the best of our knowledge, this is the first time this method has been used to obtain evidence of the use of lapis lazuli blue where a protective varnish is present.

The PIGE technique provided a direct demonstration of Leonardo's use of lapis lazuli blue in the la *Madonna dei fusi*.

## 2.3.12. *RITRATTO DI GENTILUOMO*, BY ANTONELLO DA MESSINA

A complete characterisation of the materials and the structure of paintings is hard to achieve, due to their heterogeneous nature. The composition and structure of the Ritratto Trivulzio by Antonello da Messina was characterised in a non-invasive and non-destructive way by combining PIXE, differential-PIXE (d-PIXE) and scanning-mode PIXE (s-PIXE).

At the LABEC external scanning microbeam in Florence, beam spot sizes of down to about 7 microns can be obtained on samples in a He atmosphere, by extracting the ion beam through a 100nm thick 1x1mm$^2$ $Si_3N_4$ window. A target monitoring system uses three TV cameras with adjustable magnifications for sample positioning and real time monitoring. The beam charge monitor detects Si X-rays produced by the beam in the exit window. An Ion Luminescence (IL) apparatus for the simultaneous acquisition of IL/ PIXE/ PIGE/ RBS spectra and maps is also used. IL is a natural complement of the more common IBA. This configuration is well suited to various applications in the field of Cultural Heritage.

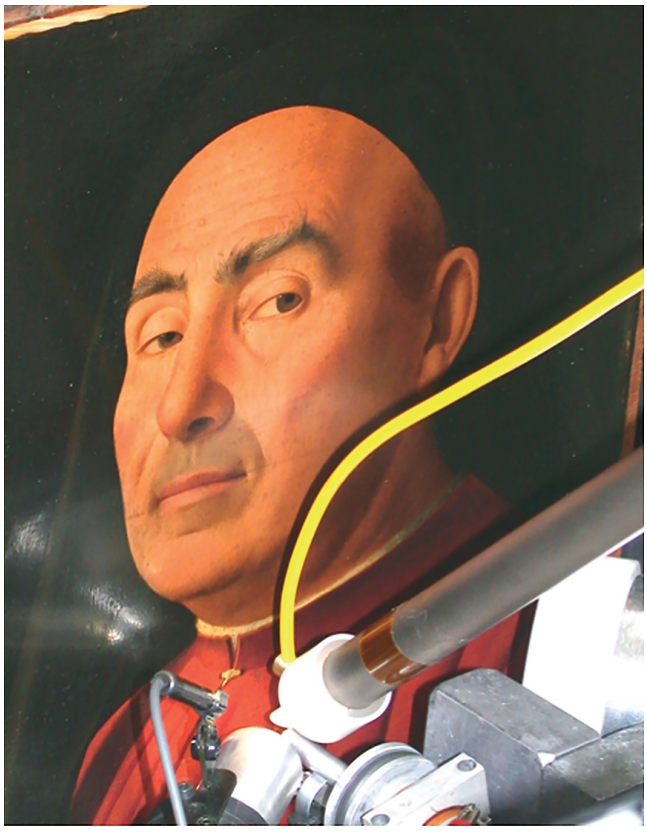

**Figure 2.17:** The painting *Ritratto Trivulzio* by Antonello da Messina (15th c.) during measurements at the LABEC external microbeam in Florence.

Extensive PIXE investigations were performed at the LABEC laboratory on the painting *Ritratto Trivulzio* by Antonello da Messina [84], one of the great Italian masters of the 15th c. and a pioneer in modern oil painting; see figure 2.17.

Non-destructive and non-invasive external beam measurements in a He atmosphere were carried out. Single-spot mode PIXE was first used for a characterisation of different areas of the painting. Then differential PIXE was used to obtain information about the layering. Finally elemental imaging, by scanning PIXE, was carried out to solve some specific problems which arose during the previous PIXE and d-PIXE studies. Here are some of the more interesting results.

The combination of PIXE, d-PIXE and s-PIXE provided information to restorers and art historians which was useful for the identification of the materials used by Antonello and to unveil some aspects of his painting technique.

- The gentleman's dark head-cloth was made of a Cu-based pigment, most likely azurite (PIXE).
- In the less dark areas of the head-cloth Pb is associated with Cu, suggesting the use of lead white (PIXE).
- The dark background was mainly composed of a Cu-based pigment (azurite) (PIXE).
- The thickness of the Cu-based layer was found to be of the order of 30–45 μm (d-PIXE).
- The presence of Sr in a deep layer was explained by hypothesising the use of calcium sulphate, a typical preparation for wood paintings (d-PIXE).
- The use of cinnabar (HgS) as the main red pigment for the mantle was apparent from all the spots analysed in this area; all spectra were indeed dominated by Hg X-ray peaks (PIXE).
- The whitish button of the gentleman's collar was made using Pb-based pigments painted over a red layer made with cinnabar (d-PIXE).
- The whole area of the mantle was very inhomogeneous (s-PIXE).

In particular, the surface was unexpectedly characterised by darker spots of sub-millimetre size.

Thanks to the use of the high spatial resolution and the imaging capabilities of s-PIXE, it was possible to ascertain that the Al and K originated from a thin layer over the cinnabar. For the restorers, this was a strong indication of the use of a red lake pigment (prepared by reaction of the organic dyestuff with potash alum) over the cinnabar. Again according to experts, the spotted effect was probably due to shrinking of the lake during drying (s-PIXE).

### 2.3.13. DATING GALILEO'S WRITINGS

Until recently (19th c.), the standard ink in Europe was iron gall ink. This ink was generally prepared by adding iron sulfate to a solution of tannic acid; see Figure 2.18. The gallotannic acid was usually extracted from oak galls, hence the name. Inks used in ancient manuscripts are characterised not only by Fe but also by other metals, most commonly Zn, Cu and Pb: their relative abundances represent a fingerprint of each particular ink. PIXE is an ideal technique to study these inks since it can provide all the required information without risk of damage to the paper.

This project focused on Galileo's folios dedicated to studies of the laws of motion [85-87]. The notes on experiments, statements of the properties of natural motion and calculations are simply notes and are undated.

There is a great interest in reconstructing the time evolution of Galileo's thought. In particular, it is of the utmost interest for the history of science to know when

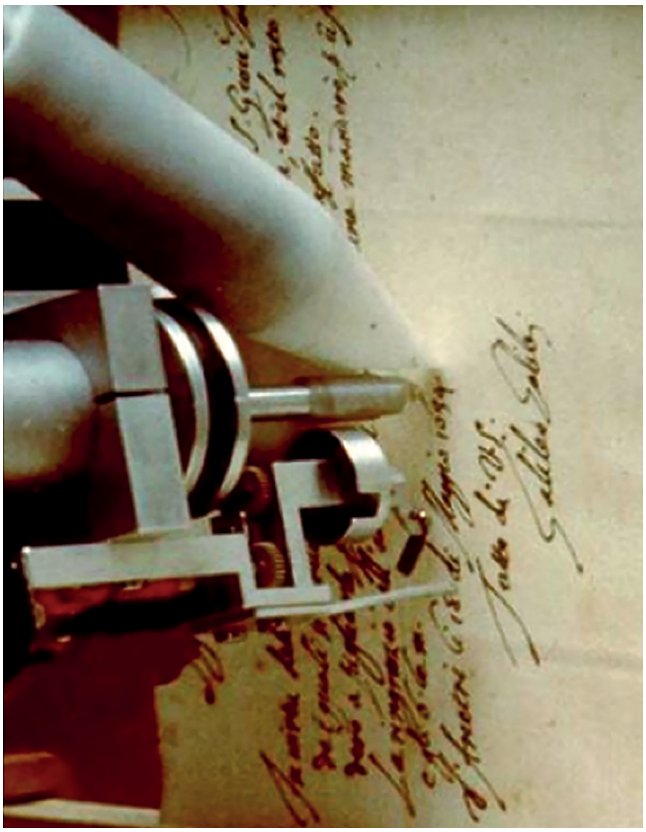

**Figure 2.18:** A letter signed by Galileo examined at the external beam PIXE set-up.

Galileo began to realise that contemporary ideas regarding the motion of falling bodies were incorrect and when he arrived at a proper description of the laws of motion.

Historians of science have dedicated a great deal of effort to reconstruct the chronology of Galileo's thoughts, basing their deductions on elements such as text analysis, handwriting and ink colour. However, there continued to be much debate about the possible dating of many documents and even about the dating of single sentences.

Radiocarbon dating, the obvious choice when dating problems are concerned, is not feasible for this task. $^{14}C$ dates have a minimum overall uncertainty of some tens of years, whereas the resolution of uncertainties in the chronology of Galileo's thoughts, requires a time resolution of a few years. In Galileo's time, ink was hand-made by apothecaries (at the time *speziali* or *drysalters*).

This explains why ink composition is expected to vary – at least in terms of relative quantities – from one batch to another. An extensive examination of dated documents (Galileo's agenda), which covered different periods of Galileo's life, was carried out to obtain ink composition profiles.

Results obtained from dated documents indicated that the elements detected were always the same at a qualitative level (S, Fe, Cu, Zn, Pb, and at times traces of Mn and light metals such as Al and Na). However, in quantitative terms, the ratios of elements related to different periods of Galileo's life are well differentiated from each other, while these ratios remain reasonably constant within short time intervals.

These results were followed by PIXE measurements on the inks of the undated folios. Inks were analysed and the composition profiles of the undated inks were obtained. By comparing the ink compositions on the dated and undated documents, it was possible to propose a tentative chronology of Galileo's writings and to resolve issues raised by previously proposed time sequences.

Here two examples of particular interest to science historians, which deal with the laws of natural motion, are reported. In the first example, the previously proposed date was confirmed by the PIXE measurements; in the second case the previously proposed date was rejected.

**First example.**
Folio 128 contains a demonstration by which Galileo reaches a correct conclusion about natural motion, starting from the wrong assumption that velocities are proportional to the distance travelled, rather than the elapsed time. Science historians had dated this demonstration to the autumn of 1604 (letter to Fra Paolo Sarpi).

In folio 128 the Pb/Fe atomic ratio is of the order of 0.5, while in all the other examined inks it never exceeds 0.025. In the entries dated from August 8 to December 24, 1604 (Galileo's agenda), the Pb/Fe ratio is about 0.5. The proposed date seems to be very reasonable!

**Second example.**
Arguing from an analogy with uniform motion, the second proposition on folio 164 verso states a wrong law of motion regarding bodies falling from the same height. The third proposition on folio 164 verso, on the contrary, clearly states the correct law of speeds. The second and the third propositions were supposed to come from the same period. All the considered ratios of elements (Cu/Fe, Zn/Fe, Zn/Cu Fe/Pb), measured on many points of the two sentences, look notably different, thus allowing for the rejection of the initial assumption.

### 2.3.14. CORROSION OF ANCIENT GLASS

The main advantage of the TOF "(Time of Flight)" spectrometer for ERDA is its capability to separate neighbouring light elements (starting with hydrogen) that recoil from the sample surface. Since ERDA is also a depth profiling technique it is widely utilised in material science applications. In contrast to NRA and PIGE that are generally applied to the analysis of specific light element isotopes, "TOF ERDA" is truly multi-elemental analysis technique. It is therefore very useful in studying samples that have a completely unknown composition as most cultural heritage objects are. The sampling depth is typically of the order of 500 nm or less, dependent on the ion mass and energy.

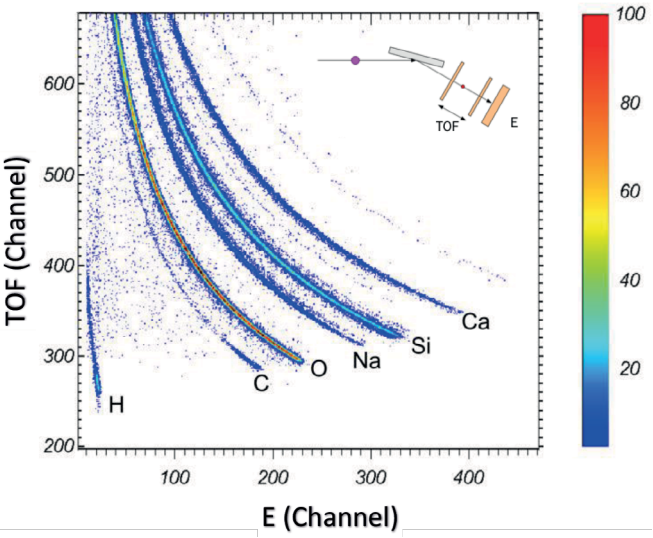


**Figure 2.19:** Two dimensional TOF-ERDA spectrum with schematic inset showing the experimental setup.

In spite of the obvious advantages, ERDA can provide useful quantitative results only if the geometry of irradiation is well defined. Samples have to be flat and, if the depth profile is required, surface roughness has to be comparable to the analysis depth. Irradiation with a heavy ion beam implies a significant energy deposition, which excludes ERDA applications from materials that are sensitive to the heat induced by the ion beam.

Alloys and glasses are among the materials that are well suited to TOF-ERDA and for which there is a need to observe changes to their surfaces when exposed to the ambient atmosphere. Unfortunately, the chemical stability of glass and several metals and alloys (*e.g.* silver) is insufficient and the appearance of such art works can be strongly affected by being exposed to different atmospheres.

Here results of the TOF-ERDA analysis of ancient glass fragments that originate from the Sokol fort in the Dubrovnik region of Croatia are presented. These fragments come from a period between the 14$^{th}$ c. and the 15$^{th}$ c. While modern glass is considered stable (*e.g.* it is used to contain acids or even to stabilise nuclear wastes), historic glass, especially medieval glass, suffers from atmospheric pollution, predominantly in recent centuries.

As seen in Figure 2.19, where a two dimensional spectrum of the energy versus time-of-flight of detected charged particles is shown, all the major elements that form glass are clearly resolved. The spectrum was recorded using a 23 MeV iodine beam with the sample positioned relative to the beam at a grazing angle of 20°. The detection system of the TOF spectrometer at the Ruder Boskovic Institute in Zagreb is positioned at an angle of 37.5° [88]. The lower edge of each individual isotope contribution in the 2D spectrum corresponds to the sample surface.

It is clearly seen that the H and C concentrations are more intense close to the surface, while Na and Ca concentrations decrease near the surface.

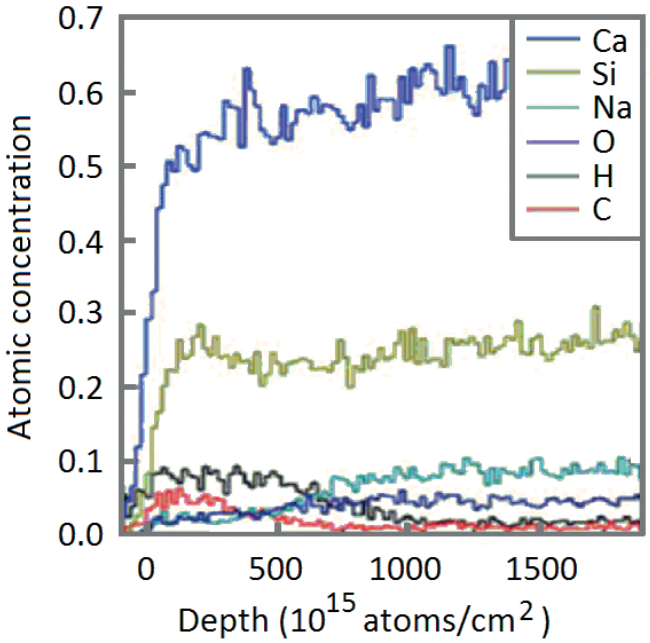


**Figure 2.20:** Depth profiles of selected elements in atomic concentration as a function of depth. $10^{15}$ atoms/cm$^2$ corresponds to approximately 0.125 nm of glass thickness.

As ERDA relies on pure Rutherford cross sections for the recoil particles, the accuracy of depth profiles is quite reliable. In this example the software package Potku [89] has been used. The results for the concentrations of different isotopes (in atoms/cm$^2$) are shown in Figure 2.20.

The observed *glass corrosion* comes from the so-called network modifiers ($Na^+$, $K^+$, $Ca^{2+}$, or $Mg^{2+}$) present in the silicate structure. When water is present on the surface and the pH is acidic (pH <7) they are extracted from the glass into the solution. In order to maintain electrical neutrality in the glass, the cations are replaced by $H^+$ or other hydrogen bearing species such as $H_3O^+$, which is exactly what has been observed in the depth profile shown in Figure 2.20.

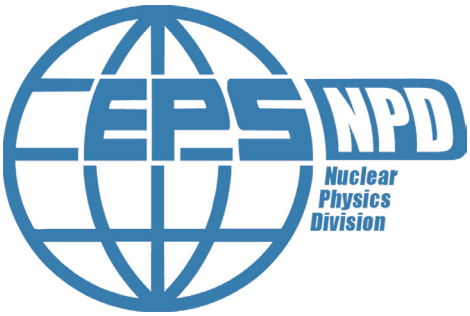


ADDRESS

6, RUE DES FRÈRES LUMIÈRE
68200 MULHOUSE – FRANCE

CONTACT

WEBSITE: WWW.EPS.ORG
PHONE: +33 389 32 94 40
FAX : +33 389 32 94 49



DOI: 10.1071/978-2-7598-2091-7

ISBN: 978-2-7598-2091-7